THE TAIWAN LIGHT SOURCE AND SUPERCONDUCTING CAVITY

G.H. Luo, Ch. Wang, L.H. Chang, M.C. Lin, T.T. Yang and C.T. Chen
SRRC, No. 1 R&D Road VI, HSIP, Hsinchu, Taiwan

Abstract

The Taiwan Light Source (TLS) is a third-generation light source with low-emittance and low operating energy, 1.5 GeV, which is used as ultra-violet and soft x-ray light source in Taiwan. Doubling the photon flux and stored beam current has been proposed to users by upgrading the RF system to superconducting cavity. The cavity's upgrading project is expected to reduce the longitudinal coupled bunch instability and increase beam lifetime by doubling the operation gap voltage. Machine status, beam parameters, RF characteristics, cryogenics system, safety issues on operation and simulation of high-power components will be presented.

1 INTRODUCTION

The Taiwan Light Source (TLS) is the first third-generation synchrotron light source in Asia located at Synchrotron Radiation Research Center (SRRC) at Hsinchu, Taiwan. Three beam lines are initially constructed when TLS opened to synchrotron users in 1993 with 1.3 GeV of nominal beam energy and 200 mA stored beam current.

Currently, there are 21 operation beam lines, two beam lines under construction and five beam lines in design or planning stage. Three branches of operation beam lines are used as diagnostic beam lines to acquire transverse beam size and the information of integral photon stability. The electron beam energy of TLS storage ring is upgraded to 1.5 GeV in 1996 [1] and full energy injection capability from booster in 2000. Basic parameters of storage ring are listed in Table 1. The schematic drawing of TLS synchrotron facility is shown in Fig. 1.

The storage ring is a six-fold symmetry Triple-Bend-Archomat (TBA) lattice with six straight sections. One section is for injection and planned to install a 3-poles with 6.5 Tesla of peak-field's superconducting wavelength shifter at downstream of the injection kicker.

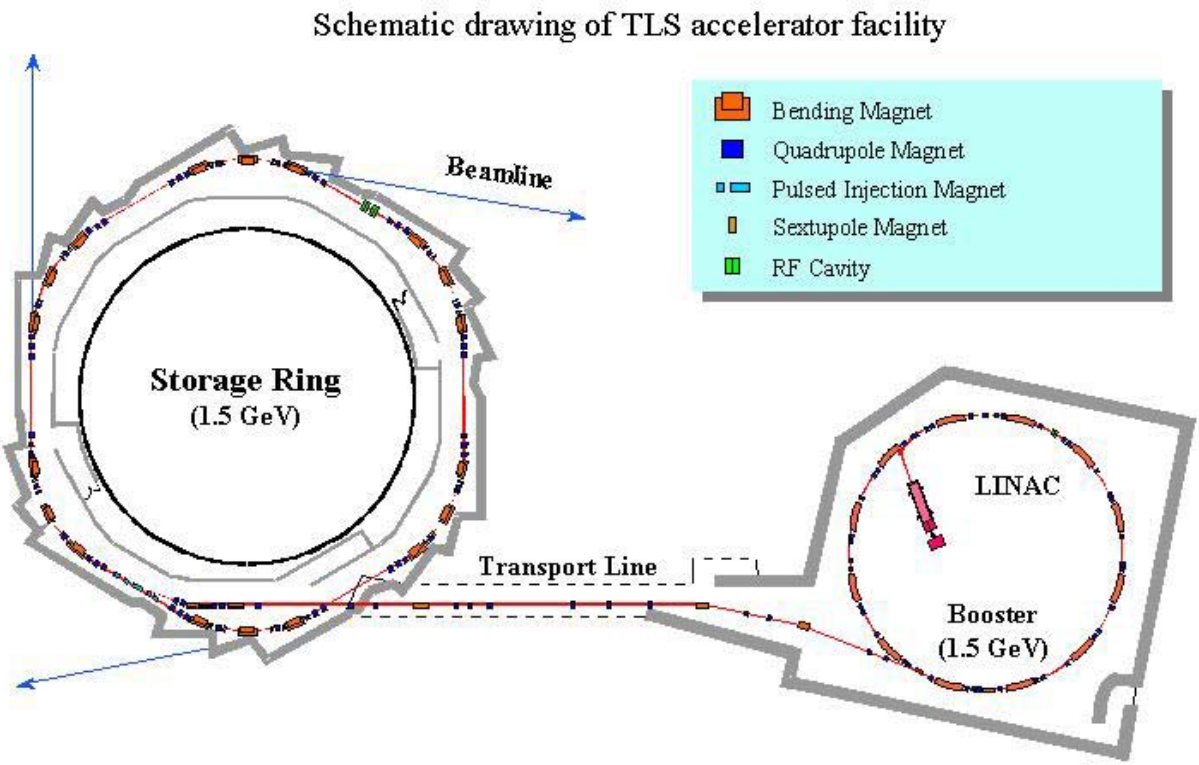

Figure 1. The schematic drawing of TLS storage ring, transport line and booster

One section is for the Doris Cavities, which will be replaced by a SRF cavity and a 29-poles' 3.5 Tesla superconducting multipoles-wiggler. The rest four sections are installed with conventional normal-conducting insertion-devices, U9, U5, W20 and Elliptical Polarized Undulator EPU5.6. Hardware parameters and radiation loss for the insertion devices are listed in Table 2. The radiation spectrum for the bending magnet, wiggler and undulators at various harmonics are shown in Fig. 2 with 200 mA stored beam current and 1.5 GeV beam energy at TLS.

Table 1. Basic parameters of the TLS storage ring

Beam Energy E	1.5 GeV
Circumference	120 m
Harmonic number	200
Working tune (H/V)	7.18/4.13
Nature chromaticity (H/V)	-15.7/-6.61
RF frequency f_{RF}	499.654 MHz
Compaction factor α	0.00678
Nature emittance ε	25.5 nm-rad.
Nature energy spread	0.000756
Operation RF voltage V_{RF}	800kV
Particle numbers (200mA/140)	$3.95*10^9$/bunch
Damping time (H/V/L)	6.96/9.37/5.67 ms
Radiation loss due to bending	128 keV/turn

Table 2. The operation parameters of insertion devices

	W20	U5	U9	EPU	SWS
Period λ_{ID} [cm]	20	5	9	5.6	~25
# of periods N_{ID}	13	76	47	6	1.5
Mini. Gap [mm]	22.5	18	18	18	18
Magnetic field [T]	1.8	0.64	1.245	0.67	6.5
Rad. Loss [keV/turn]	18.5	2.2	9.3	2.4	13.9
Total length [m]	3.04	3.9	4.5	3.9	0.625

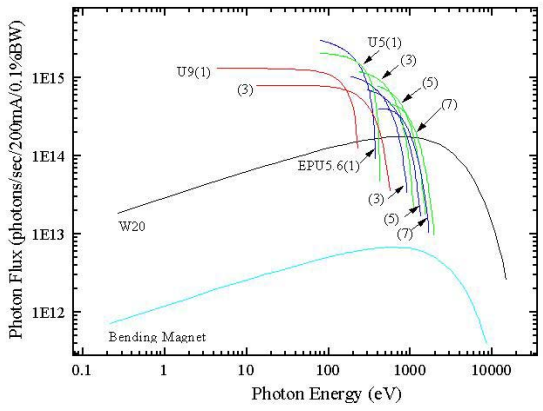

Figure 2. The spectrum for bending magnets, wiggler and undulators at various harmonics with 200 mA and 1.5 GeV electron beam at TLS.

2 PERFORMANCES OF TLS DURING USER'S SHIFT

User's beam time is scheduled 112 hours per week in normal operation period. More than 4600 hours was scheduled for users' beam time during year 2000. The operation statistics between August 2000 and July 2001 is shown is Fig. 3. Successful delivery rate to users during this period is better than 96.4%.

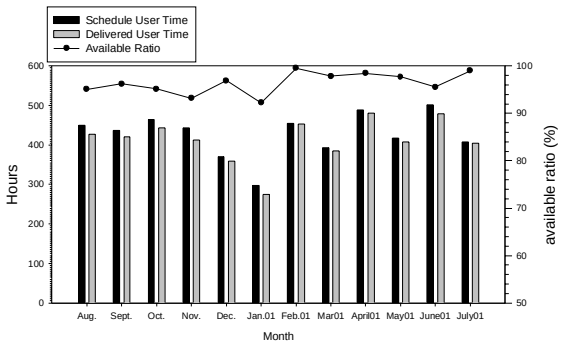

Figure 3. The statistics of users' beam time between August 2000 and July 2001. Average available ratio is better than 96.4%.

Beam stability, lifetime, current and emittance are the key parameters to the beam line users. The beam lifetime is better than 12 hours at 200 mA store beam current and the measured emittance is 20 nm-rad. The average static pressure and the dynamic pressure at 200 mA are 0.1 ntor and 0.16 ntor, respectively. The photon stability is measured through a 50 μm pinhole combined with a diode detector, which intercepts the synchrotron light focused by a vertical focusing mirror [2]. The improved cooling system of vertical focusing mirror makes the stability parameter as a reliably monitoring indicator. One of typically weekly statistics of the beam stability is shown is Fig. 4. This figure shows that there

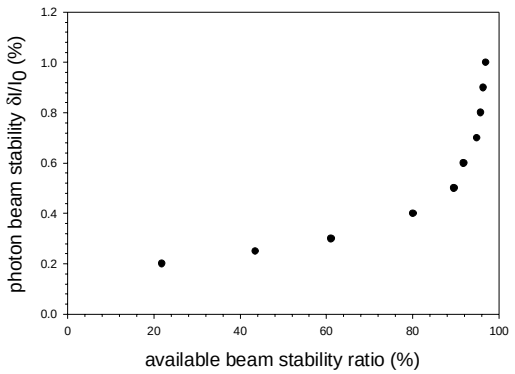

Figure 4. Beam stability ratio during users' shift

is more than 90% of users' beam time that the photon fluctuation ratio is less than 0.5%.

The temperature variation in the tunnel and the chilly-water, which is affected by the weather, the cooling capacity and operation condition, were causing long-term drift of the beam orbit. We observed a large orbit swing, more than 150 μm, at the first session of users' shift immediately after accelerator start up. It was correlated to the swing of working temperature of dipole magnets. A better temperature control of chilly water and tunnel temperature have been carried out [3] and full energy injection system also been implemented to reduce the temperature fluctuation of each injection. Figure 5 shows the beam position variation for six consecutive user's shifts currently. The average position variation is less than 10 μm among six consecutive users' shifts. The beam orbit is locked by global feedback system for individual shift. The orbit drift for each shift can be controlled down to less than 1.5 μm.

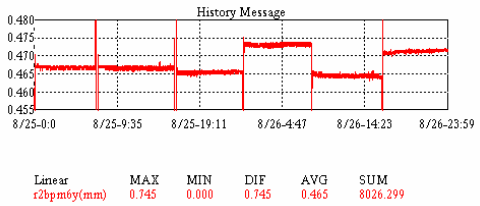

Figure 5. Beam position variation for 6-consecutive users' shifts detected by beam position monitor with resolution better than 0.1 μm.

3 DORIS CAVITY AND CESR'S CAVITY

Two Doris cavities were installed to provide proper operation power and gap voltage. A broadband loop-type damping antenna attached to the cavity cannot effectively suppress the Higher-Order-Modes (HOM). The damping antenna was replace by a plunger-type tuner in each cavity [4] to detune the most troublesome HOM. The improvement of the temperature control, ± 0.1 ^{o}C, of each cavity with dynamic range of ± 20 ^{o}C helps in suppressing the excitation of HOM. An RF gap-voltage modulation technique has also been implemented during routine operation [5]. With all of these manners, the photon fluctuation can be successfully suppressed to less than 0.3-0.4% during the users' shifters as shown in Fig. 4. However, for demanding experiments and users, the photon fluctuation is targeted to be less than 0.1% persistently. Superconducting RF cavity together with longitudinal feedback system is expected to suppress the coupled bunch instability and further reduce the photon fluctuation.

4 BEAM LIFETIME

Beam lifetime is one of the key issues in the SRF project. Touschek lifetime is a dominating factor for a low-energy synchrotron facility. The bunch length, dynamic aperture, energy acceptance and the gap voltage are the major parameters in the evaluation.

The radiation of bending and insertion devices will tend to increase the quantum fluctuations and lower the damping time. The definition of Synchrotron Radiation Integrals (SRI) constants for the operation lattice can be evaluated as reference [6]. The emittance, energy spread and bunch length can be expressed in terms of SRI. The bunch length can be expressed as:

$$\sigma_L = \left[\frac{2\pi\alpha h c^2}{\varpi_{RF}^2 \cos\phi_s}\frac{E}{eV_{RF}}\right]^{1/2}\left[\frac{55\hbar\gamma^2}{32\sqrt{3}}\frac{I_3}{2I_2+I_4}\right]^{1/2},$$

where I_1 to I_5 are SRI defined as reference [6], φ_s is the synchrotron phase and h is the harmonic number. The relationship between bunch length and gap voltage can be easily evaluated according to above equation by the assumption of operating parameters described in Table 1.

The Half-Touschek lifetime can be expressed as:

$$\frac{1}{\tau} = \frac{\sqrt{\pi} r_e c N F(\varsigma)}{\sigma_x' \gamma^3 \varepsilon_{accpt}^{\ 2} 8\pi^{1.5}\sigma_x\sigma_y\sigma_L},$$

where σ_x, σ_y, σ_L are the bunch size in x, y, and z dimension, r_e is the classical electron radius, N is the number of electrons per bunch and $\varsigma = [\varepsilon_{accpt} / \gamma\sigma_x']^2$.

The calculated Touschek lifetime by ZAP [7] for various operating gap voltages and dynamic aperture is shown in Fig. 6. From this graphs, we could find the beam lifetime will saturate around the 1.6 MV. It is an indication of a competition factor between the bunch shorting and the energy acceptance of the ring. The target operation gap voltage for TLS storage ring will be doubled from 0.8 MV, currently, to 1.6 MV for SRF cavity.

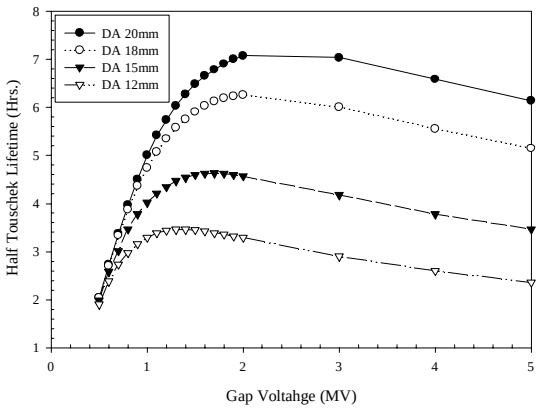

Figure 6. Half Touschek Lifetime as function of gap voltage for various dynamic apertures.

5 SRF SYSTEM

From several aspects, doubling the stored beam current, reducing couple-bunch-instability, increasing the lifetime, and compact in size, SRF cavity provides all the needs for synchrotron facility. The installation of SRF cavity will be one of the major renovations of TLS in the next decade. It will be also the first installation of SRF cavity in a dedicated synchrotron light source facility around the world. The dramatic reduction of the Q-value and shunt impedance of higher-order-mode in SRF cavity due to the large opening of beam tube will help increasing the threshold current [8]. A comparison of operation parameters for Doris cavity and CESR's SRF cavity at TLS is shown in Table 3.

The CESR's Nb cavity and cryostat is shown in Fig. 7. The round beam tube can couple most of the HOM out of the cavity. The flute-type beam tube will couple two deflecting modes (TM_{110} and TE_{111}) from the SRF cavity [9]. A rectangular waveguide is connected to the round beam tube to sever as the input coupler. Two ferrite-tiles HOM absorbers are located at the upstream and downstream of the Nb cavity at room temperature. Superconducting Nb cavity is then bath in a 4.5 K LHe vessel. The LHe vessel is insulated by vacuum, LN_2 jacket and multi-layers insulation. The earth magnetic field, 500 mG, is shield by mu-metal and cryoperm layer, hence the residual magnetic field at the equator of the Nb cavity can be guaranteed to less than 20 mG to reduce the residual resistance and cryogenic loss.

6 NUMERICAL SIMULATION OF CESR'S CAVITY

A commercial 3-D High-Frequency Structure-Simulator (HFSS) [10] is used to simulate characteristics of the RF components. The TM_{010} resonance frequency, external Q, coupling coefficient β, HOMs, and the power handling capability of ceramic window were simulated and calculated by the program. These parameters are the key factors that influence the operation of RF system and photon stability.

The full structure of CESR's cavity without input RF coupling slot has been simulated in order to find out the resonance frequency and shunt impedance of HOMs. Figure 8 shows the E-field intensity of typical higher-order mode with and without the ferrite absorber.

The 3-D model of matching rods, step changed waveguide and ceramic window was constructed to evaluate the matching condition of RF window section. The relative dielectric constant was found to be 9.6 with minimum reflection coefficient.

Table 3. The comparison of operating parameters for the Doris cavities and SRF cavity.

Parameter	Doris cavity	SRF cavity
Beam Energy (GeV)	1.5	1.5
RF Frequency (MHz)	499.666	499.666
Beam Current (mA)	200	500
Bunch Length (mm)	9.2	6.5
Energy Loss (keV/turn)	128	128 (168)
RF Gap voltage (kV)	800	1600
Number of Cavities	2	1
Number of klystrons	2	1
Wall Dissip. (W/cavity)	27.5k	<30
Beam Power (kW)	25.6	64 (84)
Klystron P_{out} (kW/kly.)	60	60 (100)
R_s/Q_0	77.441	44.5
Synchro. Freq. (kHz)	26.5	37.8
Energy Acceptance	± 1.4%	± 2.1%
RF Transmission Line	EIA6 1/8"	WR1800
Tuning Angle Offset	0^o	$0^0 > \psi_{offset} > -10^o$

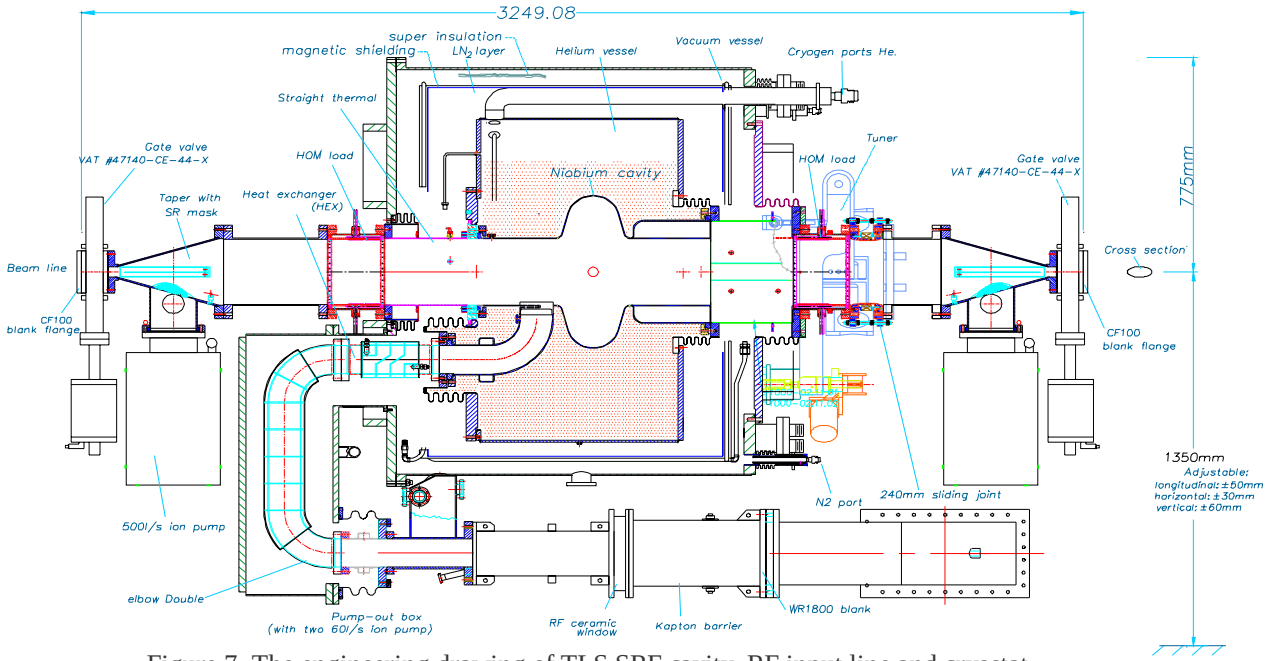

Figure 7. The engineering drawing of TLS SRF cavity, RF input line and cryostat

A sinusoid profile taper has been designed to provide a smooth transition between the cross section of RF window and the double elbow to reduce reflection coefficient. The cavity structure with input coupling section has been modeled to optimize the dimension of coupling tongue in order to find the proper coupling coefficient.

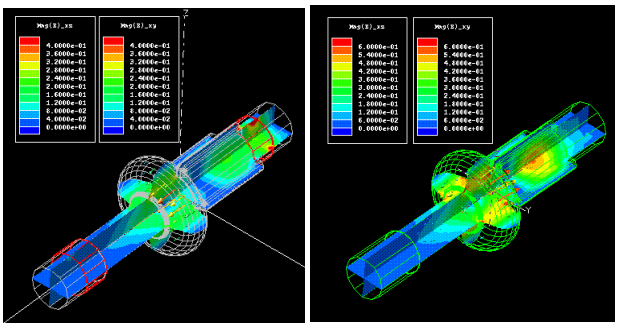

Figure 8. the HOMs with and without ferrite absorbers

7 THE CRYOGENIC SYSTEM

There is a maximum 50 Ws' heater inside the LHe vessel of cryostat in order to maintain the operation pressure and keep the cryogenic load constant as the beam current changed. Vacuum vessel, LN_2 insulation and multi-layers insulator have been used to lower the static heat loss of cryostat and distribution box.

Table 4. The estimated cryogenic budget for the transmission loss, the static and dynamic loss of cryostat.

Cryostat	2*(80 W+0.18 g/s)
Distribution Box	10 W
Multi-Channel Line (5 m)	15 W
Flexible Transfer Line	30 W
Dewar	30 W (heater)
Junctions, Valves and Misc.	40 W
Total	285 W+0.36 g/s

Two 100 m^3 and 250 psig gas helium tank will be installed nearby the compressors area. A 2000 liters liquid helium dewar is used to provide at least two times refill of LHe vessel in cryostat. The detail heat loss budget is listed in Table 4. The total heat loss plus operation margin is the capacity of desired refrigerator. It is expected to have 435 W of refrigeration capacity with LN_2 pre-cooling. Screw compressor and turbine type expander are the expected combination of cryogenic system for the reliability and easy maintenance. The turbine expander and dewar will be allocated nearby the cryostat in order to reduce the multi-channel line's heat loss.

For the first phase, the cryogenic system will provide adequate cooling capacity for the 500MHz SRF cryostat and the superconducting-multipoles-wiggler. An SC harmonic cavity is another long-term plan to increase the beam lifetime at TLS. Additional refrigerator and screw compressor should be easy to installed with current configuration to accommodate the cryogenic loss from the harmonic cavity.

8 SUMMARY

Two SRF modules and on cryogenic system were contracted to ACCEL and AIR LIQUIDE, respectively. One of two Nb cavities has competed the vertical test with satisfactory results [11]. Two RF windows have finished with high power RF processing with maximum temperature gradient less than 40 ^oC at 220 kW. Cryostats are in final assembly phase and will be tested with copper cavity insert by LN_2. The detail design review of cryogenic system is scheduled on October 2001. The scheduled commission period is the fourth quarter of 2002 and will be extended to the first quarter of 2003.

9 ACKNOWLEDGE

The authors would like to thank staff members of Beam Line Division, Instrument Development Division and Light Source Division for the valuable discussion, and suggestion at TLS. The authors are especially appreciated for the staffs, H. Padamsee, S. Belomestnykh, J. Knobloch. R.L. Geng, J. Sears, P. Quigley, J. Reilly, R. Ehrlich and M. Tigner at LNS laboratory, Cornell University, in setting up the testing system and constant guidance during our stay. The appreciation also extends to Dr. M. Pekeler at ACCEL for his dedication to this project. The HFSS simulation program is supported by National Center for High-performance Computing (NCHC) in Taiwan.

10 REFERENCE

[1] Y.C. Liu, et al., PAC'97, p.847-849, Vancouver, Canada.
[2] G.H. Luo, et al., EPAC'98, p.605-607, Stockholm, Sweden.
[3] H.M. Cheng, et al., PAC'99, p.1150-1152, New York, USA.
[4] Ch. Wang, et al., PAC'97, p.1638-1640, Vancouver, Canada.
[5] M.H. Wang, et al., PAC'99, p.2837-2839, New York, USA.
[6] R.H. Helm, et al., "Evaluation of Synchrotron Radiation Integrals," IEEE Trans. Nucl. Sci 20, p900 (1973).
[7] M.Zisman, et al., "ZAP User's Manual", LBL-21270
[8] G. Flynn, " A Comparison of the SLAC PEP-II and Cornell CESR-B Cavities for Use in the SRRC," unpublished report.
[9] S. Belomestnykh, et al., "Cutoff Frequencies of Several SRF and CESR Beam Pipe", Report 951220-18, Cornell, LNS, Ithaca, NY.
[10] HFSS, by Ansoft Corp., Pittsburgh, 1999
[11] G.H. Luo, et al., SSILS2001, to be published.